International Journal of Biological Macromolecules 145 (2020) 207–215

Contents lists available at ScienceDirect

International Journal of Biological Macromolecules

journal homepage: http://www.elsevier.com/locate/ijbiomac

Microencapsulation of sesame seed oil by tamarind seed mucilage

Erik Alpizar-Reyes, Ph. D. [a], Victor Varela-Guerrero, Ph. D. [b], Julian Cruz-Olivares, Ph. D. [a], Héctor Carrillo-Navas, Ph. D. [c], Jose Alvarez-Ramirez, Ph. D. [d], César Pérez-Alonso, Ph. D. [a,*]

[a] Departamento de Ingeniería Química, Facultad de Química, Universidad Autónoma del Estado de México, Paseo Colón esq. Paseo Tollocan s/n, Col. Residencial Colón, C.P. 50120 Toluca, Estado de México, Mexico
[b] Centro Conjunto de Investigación en Química Sustentable UAEM - UNAM, Carretera Toluca-Atlacomulco, km 14.5, Unidad El Rosedal, Toluca, Estado de México 50200, Mexico
[c] Malvern Panalytical, Laguna de Términos No. 221 - Torre A, Oficina 1403, Col. Granada, C.P. 11520 Ciudad de México, Mexico
[d] Departamento de Ingeniería de Procesos e Hidráulica, Universidad Autónoma Metropolitana-Iztapalapa, San Rafael Atlixco No. 186, Col. Vicentina, C.P. 09340 Ciudad de México, Mexico

ARTICLE INFO

Article history:
Received 3 November 2019
Received in revised form 17 December 2019
Accepted 19 December 2019
Available online 24 December 2019

Keywords:
Encapsulation
Hydrocolloid
Tamarind seed mucilage
Sesame seed oil
Spray drying

ABSTRACT

Tamarind seed mucilage (TSM) was evaluated as a novel wall material for microencapsulation of sesame oil (SO) by spray-drying method. Wall material:core ratios of 1:1 (M1) and 1:2 (M2) were considered, and the corresponding physical and flow properties, thermal stability, functional groups composition, morphology, encapsulation efficiency, and oxidative stability were evaluated. Powder of M1 and M2 microcapsules exhibited free-flowing characteristics. The particle size distribution for M1 microcapsules was monomodal with diameter in the range 1–50 μm. In contrast, Microcapsules M2 presented a bimodal distribution with diameter in the ranges 1–50 μm and 50-125 μm. M1 microcapsules were thermally stable until 227 °C and microcapsules M2 until 178 °C. Microcapsules M1 and M2 exhibited a dominant amorphous halo and external morphology almost spherical in shape. Encapsulation efficiency was 91.05% for M1 and 81.22% for M2. Peroxide formation reached values after six weeks was 14.65 and 16.51 mEq/kgOil for M1 and M2 respectively. Overall, the results led to the conclusion that tamarind mucilage is a viable material for high microencapsulation efficiency, while offering protection against oxidation mechanisms of SO.

1. Introduction

New consumer trends have promoted a noticeable growth in the demand of sustainable, eco-green and minimally processed food ingredients. Concomitantly, the search, development, and application of new techniques and formulations of active and healthy products, using natural and active compounds have intensified in the recent decade. In this way, actual industrial production of food products is more complex, involving the inclusion of bioactive compounds with potential health benefits. However, the stability of bioactive compounds is a critical parameter for their successful incorporation into various food systems [1,2]. Hydrocolloids are widely used in food matrices for the protection of active ingredients. Commonly, natural polysaccharides are the basic bricks for the fabrication of hydrocolloids [3,4]. Entanglement of linear and branched polysaccharide chains, electrostatic forces and weak hydrogen bridging are mechanisms involved in the formation and stabilization of hydrocolloids. Gums (e.g., Arabic), chitosan, starch are instances of polysaccharides that have been extensively considered for food hydrocolloids.

The recent decade has witnessed the search of polysaccharides from novel botanical sources as a supplementary alternative for traditional materials. The motivation relies on promoting sustainable and renewable exploitation of natural resources in tropical and sub-tropical regions. In this regard, mucilages from aside residues of food commodities have been explored for utilization in food hydrocolloids. Besides polysaccharides, mucilages contain functional compounds with potential benefits for human health [5]. Interestingly, mucilages extracted from seeds can be obtained at relatively low costs while offering a low-calorie intake [6,7].

Tamarind is a potential source of polysaccharides with application in food matrices. It has been reported that tamarind seed contains ~72% of mucilage, which can be obtained as a by-product of the tamarind pulp industry. Tamarind seed mucilage is composed of β-(1,4)-D-glucan backbone substituted with side chains of α-(1,4)-d-xylopyranose and (1,6)linked [β-D-galactopyranosyl-(1,2)-α-D-xylopyranosyl] to glucose residues, where glucose, xylose and galactose units are present in ratios of 2.8:2.25:1.0 as the monomer units and with a molecular weight of 720–880 kDa [8]. Previous studies have explored the chemical, physical, thermal, thermodynamic, rheological and functional properties of tamarind mucilage [6,7], showing its valuable potential functional and a low-cost source of wall material to be applied on encapsulation of food ingredients.

* Corresponding author.
E-mail addresses: ealpizarr@uaemex.mx (E. Alpizar-Reyes), cpereza@uaemex.mx (C. Pérez-Alonso).

https://doi.org/10.1016/j.ijbiomac.2019.12.162
0141-8130/

Encapsulation is often required for lipids of nutritional interest, especially lipids that are unsaturated and therefore particularly prone to oxidation and other degradation. The most interesting oils that have been explored in food science are those with high omega-3 fatty acid content. These oils have been touted for their health benefits but are currently typically consumed in the form of a large capsule that can be difficult to swallow and lead to fishy breath and repeating. A suitable solution is to find a way for incorporating oils into small microcapsules by spray drying and subsequently adding the resulting product into food and beverage products [1]. Sesame seed oil (SO) has been used as a natural ingredient in salads and as a seasoning oil to prepare foods. The main compounds of the sesame oil are unsaturated fatty acids (UFA), ~47% of linoleic acid and ~37% of oleic acid [9]. In the last years, it has been reported that the consumption of sesame oil has positive effects in blood lipid profiles, increasing anti-inflammatory function, and exhibiting antimutagenic activity [10]. Unsaturated essential fatty acids in SO are chemically unstable in presence of oxygen, light, moisture and heat. However, this problem can be fixed by enhancing the stability of SO through microencapsulation process by spray drying. To this end, the proper selection of a wall material is a central issue. In particular, a suitable wall material should exhibit high encapsulation efficiency and protection against oxidation mechanisms of oils along time. Nowadays, there are only some studies focused on proving the application of mucilages employing adjuvants (e.g., gums and proteins) as wall materials to encapsulate some lipids prone to oxidation [11–14]. However, studies dealing with the sole use of mucilages as wall materials in the microencapsulation processes have not yet been published.

The aim of this work was to introduce tamarind seed mucilage as a wall material without any other hydrocolloid for spray-drying microencapsulation of sesame seed oil susceptible to degradation processes. Besides, the resultant microcapsules with sesame seed oil were characterized for their physical and flow properties, thermal stability, functional groups composition, morphology, encapsulation efficiency, and oxidative stability.

2. Materials and methods

2.1. Materials

Sesame seeds were purchased at a local market (Toluca, Mexico). Tamarind seed mucilage was extracted according to a method previously reported [8]. Chemical reagents were purchased from Sigma Aldrich S.A. de C.V. (Toluca, Mexico). Bidistilled water was used in all experimental runs.

2.2. Oil extraction

A Tamer hydraulic press (Model PT-20, Shanghai, China) fitted with a 40 cm long and 10 cm diameter plunger was used for cold pressing sesame seeds in order to extract seed oil. The maximum pressure applied by the piston was 8.8×10^8 N/m^2, at room temperature (~20 °C). Sesame seed oil (SO) was stored in amber bottles at ~4 °C for further measurements.

2.3. Emulsions preparation

Aqueous stock solutions of tamarind seed mucilage (TSM) with 0.3% w/w sodium azide to prevent the proliferation of microorganisms, were prepared and kept overnight in a shaking water bath at ~40 °C, to warrant full hydration of the biopolymer molecules. Stock solutions of TSM were used as wall materials, and sesame seed oil (SO) were used as core material. Two oil-in-water emulsions (O/W) were formulated. The first one (E1) with wall material:core ratio (Wm:Co) of 1:1 in dry basis, a total solid content of 10% w/w and a $\phi_{O/W} = 0.05$. The second one (E2) with wall material:core ratio (Wm:Co) of 1:2 in dry basis, a total solid content of 15% w/w and a $\phi_{O/W} = 0.1$. E1 and E2 were made by adding the required amount of oil and pouring dropwise into the prescribed amount of TSM at ~30 °C. Emulsification was carried out with an Ultra-Turrax T50 homogenizer (IKA®-WERKE Works Inc., Wilmington, NC, USA) at 6400 r.p.m. during 10 min. The emulsions were maintained in a water bath with the purpose of keeping the temperature below 30 °C.

2.3.1. Emulsifying properties

The emulsifying stability and activity were determined based on the method proposed by Alpizar-Reyes et al. 2017 [6]. To this end, the emulsions E1 and E2 were centrifuged with a Hermle Z323K highspeed centrifuge (Hermle, Labortechnic, Germany) for 10 min at 524 ×*g*. The emulsifying ability (EA) was calculated as follows:

$$\%\ EA = \frac{Emulsion\ \ volume}{Total\ \ volume} \times 100 \tag{1}$$

Emulsifying stability (ES) was evaluated with a method similar to the EA method [6]. After the emulsions were homogenized, they were heated in a water bath at 80 °C for 30 min, and subsequently cooled down to room temperature (20 ± 2 °C), and centrifuged for 10 min at 524 ×*g*. The emulsified layer was measured, and the ES calculated using the following equation:

$$\%\ ES = \frac{Final\ \ emulsion\ \ volume}{Initial\ \ emulsion\ \ volume} \times 100 \tag{2}$$

The creaming index (CI) was evaluated as described by Manoi and Rizvi [15] with some adaptations. 10 mL of each emulsion was filled into a glass test tube (1.5 cm internal diameter and 12 cm height) and then stored at room temperature (20 ± 2 °C). The height of the serum (H_S) and the total height of emulsions (H_T) were recorded after storage at ambient temperature for 1, 7, 14 and 21 days. The creaming index was reported as:

$$\%\ CI = \frac{H_S}{H_T} \times 100 \tag{3}$$

2.4. Spray drying of emulsions

The emulsions were fed at a rate of 40 mL/min to a Nichols/Niro spray-drier (Turbo Spray PLA, NY, USA) operated with an inlet temperature of 135 ± 5 °C, outlet temperature at 80 ± 5 °C and injecting compressed air at 4 bar [7]. The spray-dried emulsions E1 and E2 after the drying process turned into microcapsules M1 and M2, respectively. Then, microcapsules were stored in desiccators above P_2O_5 to prevent any increase in absorbed moisture, until they were required for experiments.

2.5. Physical properties of microcapsules

2.5.1. Bulk and tapped densities

Bulk density was measured by transferring 20 g of microcapsules into a graduated measuring cylinder and the volume occupied by the microcapsules gave the bulk volume. The measuring cylinder was clamped to the USP 1 tapper (USP Toron Pharma – TD10, Ontario, Canada). Tapped density was measured by mechanically tapping the measuring cylinder containing microcapsules until the constant volume was observed up to 600 taps. Bulk and tapped density were calculated as the ratio of the mass of the mucilage to the bulk or tapped volume, respectively [16].

2.5.2. Compressibility index

The compressibility index of the microcapsules was determined according to the Carr's index as follows [16]:

$$\text{Carr's Index} = \frac{\text{Tapped Density} - \text{Bulk Density}}{\text{Tapped Density}} \times 100 \quad (4)$$

2.5.3. Hausner's ratio

The Hausner's ratio was determined by the ratio of tapped density and bulk density based on following equation [16]:

$$\text{Hausner's Ratio} = \frac{\text{Tapped Density}}{\text{Bulk Density}} \quad (5)$$

2.5.4. Moisture content

The moisture content of TSM microcapsules M1 and M2 was determined according to the AOAC standard method 925.10 [17]. Briefly, the moisture content of TSM microcapsules was determined gravimetrically by oven-drying at 105 °C up to constant weight using 1 g of powder and the moisture was expressed in terms of percentage on dry basis. For all physical properties, measurements were made for at least three duplicates of each sample.

2.6. Physicochemical analysis

2.6.1. Fourier transform infrared spectroscopy (FTIR)

Functional groups of microcapsules were determined using Fourier transform infrared spectroscopy (FTIR) using a spectrophotometer FT-IR GX System (Perkin–Elmer, Shelton, CT, USA) coupled to an ATR DuraSample II accessory. All the spectra were an average of 16 scans from 36,500 to 800 cm^{-1} at a resolution of 2 cm^{-1}.

2.6.2. Thermogravimetric analysis

The thermal characteristics of the microcapsules were studied using thermogravimetric analysis (*TGA*). *TGA* studies were carried out using a TA-DSC Q1000 calorimeter (TA-Instruments, New Castle, DE, USA) equipped with a mechanical refrigeration system (RCS-refrigerated cooling accessory), with a heating ramp of 2 °C/min. Samples were heated from 0 °C to 400 °C. Aluminium crucibles of 5 mm diameter were used. The instrument was purged with nitrogen at a flow rate of 100 cm^3/min. The data were analyzed using Universal Analysis 2000 software, version4.7a (TA Instruments, New Castle, USA).

2.6.3. X-ray diffraction

X-ray diffraction (XRD) patterns of microcapsules were obtained using a diffractometer Siemens D4 (Endeavor, Bruker AXS GmbH, Karlsruhe, Germany) with Co-Kα radiation. Diffractograms were taken between 5° and 55° (2Θ) at a rate of 1°/min (2Θ) and with a step size of 0.05° (2Θ). The diffractrograms were obtained at 25 °C using an accelerating voltage of 15 kV and a current of 40 mA. For all the physicochemical characteristics, measurements were made with at least three replicates of each sample.

2.7. Encapsulation efficiency

2.7.1. Surface oil content

The surface oil in microcapsules was determined by means of the method proposed by Rodea-González et al. [18], with some modifications. Briefly, 5 g of microcapsules were dispersed in 50 mL of n-hexane followed by 10 min stirring. The suspension was filtered, and the residue was washed three times with 5 mL of n-hexane. The obtained powder was dried in an oven at 80 °C until the weighed mass was constant (W). The surface oil in microcapsules was determined to calculate the difference between the initial microcapsules mass and the powder mass obtained after drying (W).

2.7.2. Total oil content

Total oil content was measured according to Rodea-González et al. [18], with some modifications. Briefly, a suspension formed through the dispersion of 5 g of microcapsules into 180 mL petroleum ether was sonicated on an ice bath for 5 min at an amplitude of 50% and a frequency of 30 kHz. The oil was extracted using a Soxhlet (VLP-SER 148/6) system, with an extraction time of 6 h. After extraction, the powder was dried until constant mass. The total content of oil was calculated as the difference between the initial mass of microcapsules and the powder mass obtained after extraction with Soxhlet.

2.7.3. Encapsulation efficiency

The encapsulation efficiency was calculated using the following equation:

$$\text{EE } (\%) = \frac{\text{Total Oil} - \text{Superficial Oil}}{\text{Total Oil}} \times 100 \quad (6)$$

For all the encapsulation efficiency studies, at least three duplicates of each sample were analyzed.

2.7.4. Lipid oxidation by peroxide value

For oxidation assessment, microcapsules and free oil were stored at 25, 35 and 40 °C and water activities of 0.329, 0.318 y 0.313, respectively, to each temperature. To achieve those conditions, microcapsules and free oil were spread in pans of 3.5 cm of diameter (surface area of 9.6 cm^2) and stored in sealed containers in order to accelerate the oxidation process. The headspace for both microcapsules and free oil samples was 4 cm. For each time point of analysis, one sealed container was removed. The contents were analyzed and then disposed to prevent new oxygen being introduced after sampling. Samples were not exposed to light during storage. Once the storage conditions were achieved, a sample of 1.0 g of microcapsules was dissolved in 10 mL of water. A 400 μL portion of the dissolved microcapsules was mixed with 1.5 mL of an isooctane/isopropanol (1:2 v/v) solution, which then was vortexed three times for 10 s [19]. The phases were separated, and the upper phase was taken for further analysis. The peroxide value corresponding to microencapsulated as well as free oil was determined spectrophotometrically. A 400 mL portion of extraction medium (or 0.2 g in the case of free oil) was added to 9.6 mL of a chloroform/methanol (7,3 v/v) mixture. For color formation, 50 mL of an ammonium thiocyanate/iron (II) chloride solution was added. The sample was vortexed for 4 s. The absorbance of the samples was read at 510 nm after 20 min reaction time using the UV–Vis spectrophotometer model Genesis 10 (Thermo Scientific, Waltham, MA), and hydroperoxide concentrations were determined using a standard curve of cumene hydroperoxide [20]. For lipid oxidation by peroxide studies, at least three duplicates of each sample were analyzed.

2.8. Surface and size of microcapsules

2.8.1. Scanning electron microscopy analysis

The surface morphology of the microcapsules by SEM was acquired using a JSM-6510 model scanning electron microscope (Jeol Co. Ltd., Tokyo, Japan) with a voltage acceleration of 15 kV. The samples were mounted on circular aluminium stubs with double-sided sticky tape, coated for 250 s with 15 nm gold. Micrographs at 1000× magnifications were presented.

2.8.2. Particle size distribution

The particle size distribution was analyzed in a particle size analyzer Malvern Mastersizer 3000 packed with an unity for powders AERO S and operated with a software Mastersizer 3000 version 3.63 (Malvern

Instruments Ltd., Malvern, Worcestershire, UK) which was used to determine the volume-weighted mean size ($D_{[4,3]}$) of the microcapsules. The refractive index used was 1.39; the adsorption index was 0.1 and the air pressure was 4 bar.

2.9. Statistical analysis

Data were analyzed using a one-way analysis of variance (ANOVA) and a Tukey's test for a statistical significance $P \leq 0.05$, using the software Minitab 17. All experiments were done in triplicate.

3. Results and discussion

3.1. Emulsifying properties of emulsions

Emulsifying activity measures the ability of an emulsifying agent to form water-in-oil emulsions, whereas the emulsion stability measures the break-down process over time. Emulsifying activity was greater for emulsion E2 (Table 1) than E1, because there was a greater presence of retained oil within the emulsion oil drops. The effect can be explained by the presence of long chains of the branched structure of tamarind seed mucilage on the surface active to absorb oil molecules lower the surface tension [6]. On the other hand, emulsifying stability for E2 decreased with respect to E1, an effect that might be due to the higher core:ratio for E2. Also, the reduction of surface tension of tamarind seed mucilage on E2 might lowered the stability in time. The creaming index has been used to indicate the susceptibility of oil droplets to coalescence by forces such as gravitational, colloidal, hydrodynamic, and mechanical, and the resistance of the droplet membrane to rupture during a certain period of time [21]. As depicted in Table 1, E2 emulsions showed higher creaming values and a bigger phase separation, whereas the creaming index of emulsions was dependent of oil retained into emulsion. Clearly, the emulsion stability was reduced by increasing the amount of oil in emulsions.

3.2. Physical properties of microcapsules

3.2.1. Bulk and tapped densities

The results of bulk and tapped densities are shown in Table 2. Bulk density is an important property for assessing packaging, good reconstitution, and retail use of microencapsulated powders. Bulk density is dependent on the degree of inter particulate space or porosity of the bulk volume. Bulk density values varied in the range from 0.26 to 0.28 g/mL for both M1 and M2. These values are in accordance with the values commonly observed for microencapsulated powders. The low bulk density values for M1 can be attributed to the reduced content of sesame seed oil present in the microcapsules. This feature helps to achieve a higher degree of occupation of TSM as a barrier agent. In fact, it is well-known that the prevalence of barrier agents promotes the spongy nature of microcapsules [22]. A further explanation for the lowest bulk density could be linked to the fact that the bulk density decreased when the diameter of the particles decreased [23]. A useful parameter affecting the design variables (e.g., transportation, packaging and commercialization of microcapsules) is the tapped density, which determines the weight and amount of powder that can be placed into a container. M2 exhibited higher values for tapped density that M1. The amount of oil encapsulated and final concentration on M2 was higher than M1 and impacted on the tapped density with higher values. The production of spray-dried microcapsules with higher tapped density will require the use of smaller containers, representing a great advantage for manageability. Furthermore, higher bulk density indicates a lower amount of air presented in the powder, which can help to prevent lipid oxidation during storage [22].

Table 1
Emulsifying properties for TSM-SO microcapsules.

	E1	E2
Emulsifying activity (%)	86.26 ± 0.03^a	90.28 ± 0.02^b
Emulsifying stability (%)	82.31 ± 0.04^a	80.33 ± 0.13^b
Creaming index (%)	9.87 ± 0.14^a	11.79 ± 0.09^b

Values are means ± standard error, of three replicates. Superscripts with different letters in same row indicate significant differences ($P \leq 0.05$).

Table 2
Physical properties of TSM-SO microcapsules.

	M1	M2
Bulk density (g/mL)	0.26 ± 0.03^a	0.28 ± 0.02^a
Tapped density (g/mL)	0.31 ± 0.04^a	0.33 ± 0.13^a
Carr index (%)	13.79 ± 0.14^a	15.57 ± 0.09^b
Hausner radius	1.16 ± 0.02^a	1.19 ± 0.04^b
Moisture content (% w/w)	4.07 ± 0.12^a	6.32 ± 0.07^b
Surface oil (%)	8.81 ± 0.08^a	16.89 ± 0.06^b
Encapsulation efficiency (%)	91.05 ± 0.05^a	81.22 ± 0.03^b

Values are means ± standard error, of three replicates. Superscripts with different letters in same row indicate significant differences ($P \leq 0.05$).

3.2.2. Flowing properties

Carr index (compressibility percentage) and Hausner ratio are the most common parameters used to describe the flowing properties of microcapsules in powder form. In agreement with Turchiuli et al. [24], compressibility percentages (Carr index values) between 11.0 and 15.00 indicate powders with good flowability, which are characteristic of free-flowing powders. For M1 and M2 microcapsules, values from 13.79 to 15.57% of compressibility were obtained. In turn, this indicates that free-flowing powders were present, which would not require the addition of flowing promotors. It has been reported that higher oil contents on microcapsules exert a negative influence on the bulk density of the powder and consequently impacts on the flowability of the microcapsules [23]. In turn, this characteristic promotes a reduction on the flowability of the microcapsules. The effect was observed for M2 microcapsules with lower flowability compared with M1 microcapsules.

Other useful parameter to characterize the flowability of microcapsules is the Hausner ratio, which evaluates the cohesiveness of the powder. Values close to 1.0 indicate the good ability of powders to flow; while values >1.60 denote awful flow properties. In this way, a higher Hausner ratio indicates that the powder is more cohesive and less able to flow freely. For M1 microcapsules, the Hausner ratio was 1.16, indicating good flowability. However, for M2 microcapsules Hausner ratio was 1.19, just on the limit for having good flowability, indicating fair flowability [23]. The small difference of Hausner ratio between M1 and M2, might be due to the amount of superficial oil in M2 (Table 2). This fact would reduce slightly the flowability of powder given the tendency to agglomerate.

The moisture content of the microcapsules ranged from 4.07 to 6.32% w/w (Table 2). This means that microcapsules exhibited moisture contents that allow free flow behavior with no need of adding flow promoters during formulation processing.

3.3. Physicochemical analysis

3.3.1. Fourier transform infrared spectroscopy (FT-IR)

Fig. 1 shows the FT-IR spectra of microcapsules prepared with tamarind seed mucilage (TSM). Microcapsules M1 and M2 showed similar spectra peaks. Two notable regions corresponding to wavenumbers of 3600–2700 cm^{-1} (mainly linked to lipids) and 1800–800 cm^{-1} (linked to proteins and carbohydrates) were obtained. Strong characteristic bands of lipids in the high wavenumber region (3000–2800 cm^{-1}), including duplets centered at 2920 and 2850 cm^{-1} and single peaks located at wavenumbers of 1743 and 1415 cm^{-1}, are attributed to the sesame seed oil (SO) contained on the microcapsules. The duplet (2920 and 2850 cm^{-1}) bands are attributable to ν(C—H) stretching

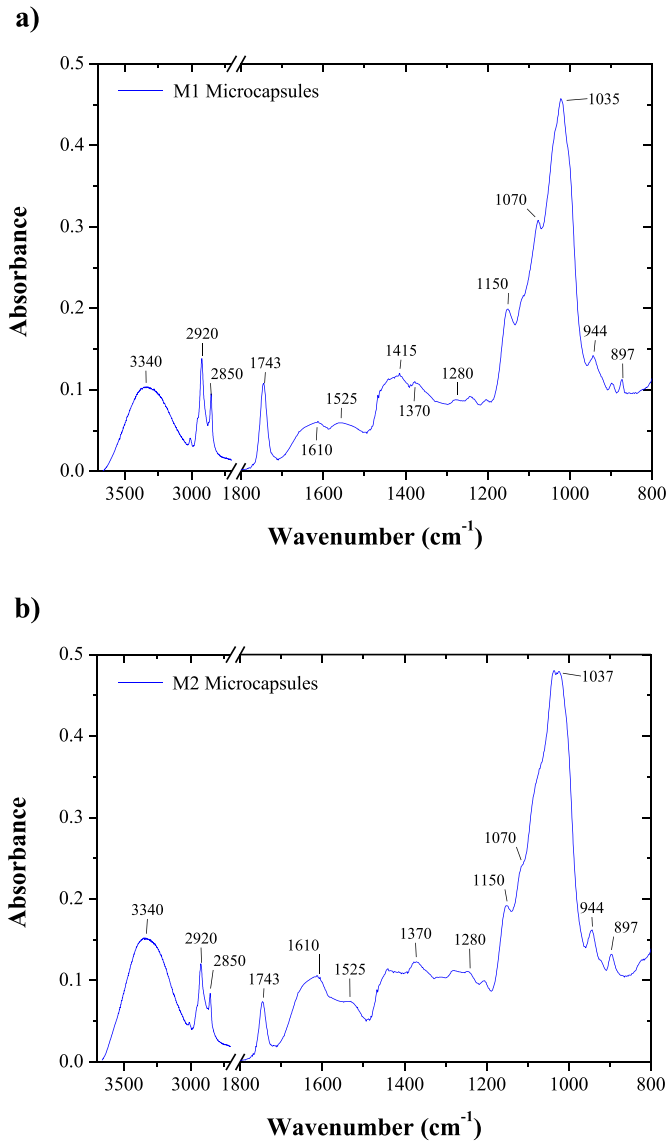

Fig. 1. Fourier transform infrared spectroscopy (FTIR) of TSM-SO microcapsules.

modes of the methyl (−CH3) and methylene (−CH2) backbones of lipids (symmetrical and asymmetrical, respectively). In particular, the peak at 2920 cm^{-1} is associated with ν(C—H) stretches of cis-alkene (−HC=CH−) in unsaturated fatty acids (UFAs), consequently, represents the midst of the UFA in the sample [25]. The position of this peak can be used to determine the degree of unsaturation in fats and oils because the higher the number of olefinic double bonds (–HC=CH–) presented in the fatty acid molecules, the higher the wavenumber of the peak. Similarly, the presence of this peak at a lower wavenumber suggests a lower degree of unsaturation in the lipid contents of the examined material. In addition, the sharp peak at 1743 cm^{-1} assignable to ν(C—O) stretches of ester functional groups from lipids and fatty acids is typically indicative of total lipids in most biological compounds [26,27]. The peak at 1415 cm^{-1} is referred to the combination of deformation modes of methyl (−CH3) and methylene (−CH2) groups in the lipid structures [25]. Meanwhile, peaks at 3340, 1610, 1525, 1370, 1280, 1150, 1070, 1035, 944 and 897 cm^{-1} correspond primarily to the isolated tamarind seed mucilage (TSM). The wide strong peak of absorption in the region of 3340 cm^{-1} is the most notable peak that denotes the interaction between TSM and sesame seed oil, it is attributed to the overlapping deformation modes of =C-O stretch, which corresponds to the lipid fraction of tamarind seed mucilage and the presence of slight interactions with sesame seed oil [6]. For the second region, the band at 1610 cm^{-1} is linked to -C=O stretching characteristic of Amide I from proteins of the acetylated units (-$CONH_2$ groups). The band at 1525 cm^{-1} corresponds to the Amide III (-NH_3^+ groups), and the band at 1280 cm^{-1} has been attributed to the stretching of the C—O bond [6].

Peaks at 1370, 1150, 1070, 1035, 944 and 897 cm^{-1} are characteristic absorbance peaks of the xyloglucan commonly observed on the xyloglucan backbone [28], which is the most important component of TSM. The peak at 1370 cm^{-1} represents the CH_2 bending of xyloglucan, and a soft peak located at 1150 cm^{-1} is related to the O-C-O asymmetric stretching. Moreover, the bands observed at 1037 and 1071 cm^{-1} are assumed as resulting from C—O and C—C stretching of the xyloglucan ring. The peak at 944 cm^{-1} denotes the ring vibration of xyloglucan. Finally, the band at 897 cm^{-1} corresponds to the C—H stretching representative of glucose and xylose β-anomeric links of TSM [6,29]. Despite the FT-IR spectra of the M1 and M2 microcapsules, typical signals were observed for major components of both systems, i.e., sesame oil, xyloglucan, glucose and xylose, those interactions were not significant enough to cause peak shifts, as it is illustrated in Fig. 1.

3.3.2. Thermogravimetric analysis

The results of thermogravimetric analysis (TGA) for M1 and M2 microcapsules are shown in Fig. 2. It can be seen that two main stages of mass loss were displayed. The first mass change can be associated with the loss of moisture correspondent to adsorbed and structural water. For M1, the first mass change of 2.54% is observable at temperatures between 20 and 75 °C; meanwhile, for M2 the event occurred at temperatures between 14 and 68 °C with loss of 4.96%. In turn, this transition is associated with the hydrophilic nature of the functional groups of each polysaccharide of tamarind seed mucilage [6]. The second mass change, for M1 was of 74.96% at temperatures up to 227 °C, while for M2 it was 77.04% at temperatures higher than 178 °C. This second mass loss has been attributed to the polysaccharide thermal decomposition corresponding to tamarind seed mucilage and superficial sesame seed oil. The difference of temperatures between M1 and M2 at which occurs mass loss events could be attributed to the amount of oil used on each formulation since oils are highly susceptible to mass loss at low temperatures. Similar ranges of weight loss were observed for cactus mucilage used as an encapsulating agent [30].

3.3.3. X-ray diffraction

XRD was performed to confirm the amorphous structure of microcapsules. The regular arrangement of atoms and molecules produces

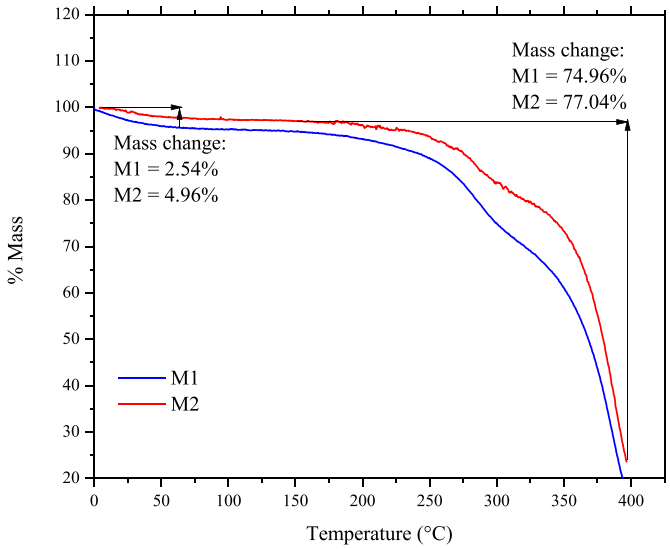

Fig. 2. Thermogravimetric analysis for TSM-SO microcapsules.

sharp diffraction peaks, whereas amorphous regions result in broad halos. X-ray diffraction patterns of M1 and M2 are shown in Fig. 3a and b, indicating a dominant amorphous halo with a broad band centered at 2θ = 20°. Previous studies have also shown the amorphous nature of tamarind seed mucilage with a broad band centered at 2θ = 20° [6]. Moreover, it has been demonstrated that bulk sesame seed oil also shows a broad halo at 2θ = 20° [31], contributing to the amorphous nature of the microcapsules system.

3.4. Encapsulation efficiency

3.4.1. Surface oil content and encapsulation efficiency

Table 1 presents the surface oil content and encapsulation efficiency for TSM-SO microcapsules. The surface oil was significantly higher for M2 microcapsules (16.89%) than for M1 microcapsules (8.81%). In the latter case, the surface oil content was drastically reduced, which is important to provide storage stability of the encapsulated material. This phenomenon can be explained from the lower amounts of barrier agent employed on M2 microcapsules. In fact, increased material content allows a better coating of oil droplets before drying process [32]. On the other hand, encapsulation efficiency presented greater values for M1 microcapsules (91.05%) than for M2 (81.22%) microcapsules.

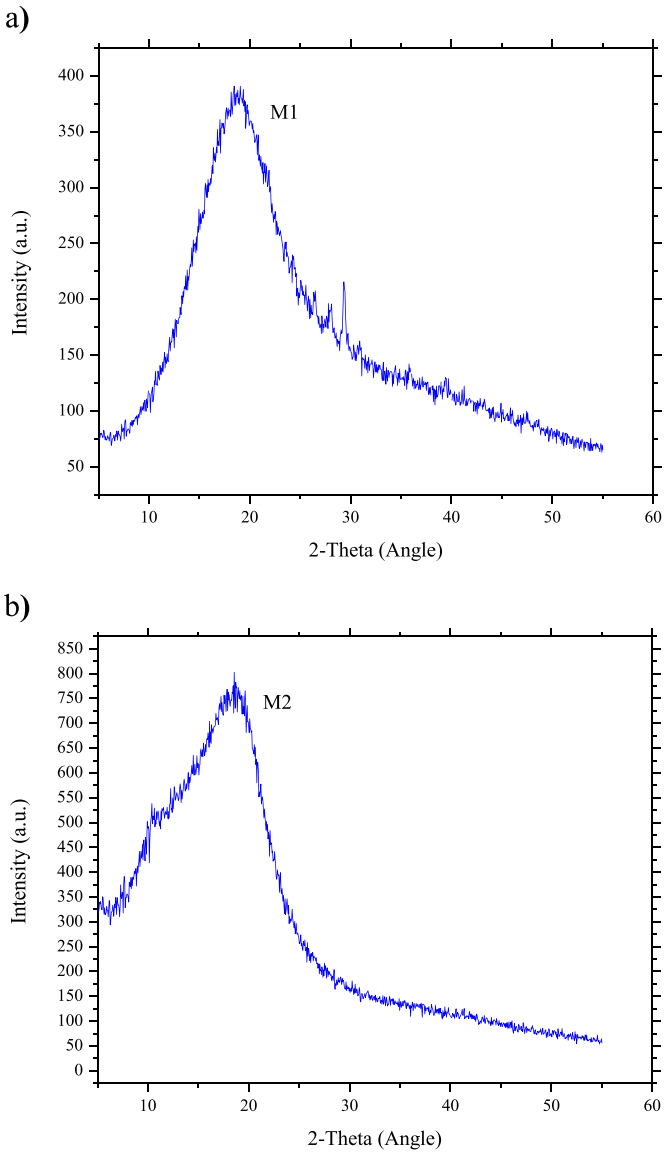

Fig. 3. X-ray diffraction studies of a) M1 and b) M2 microcapsules.

Hence, the most ideal system among this study was M1, leading to the optimal encapsulation efficiency for the microencapsulation of SO with the lowest proportion of surface oil. Encapsulation efficiency was affected significantly by Wm:Co ratio since when such ratio increased from 1:1 to 1:2, the encapsulation efficiency decreased and surface oil increased (Table 2). As the ratio of wall material:core was increased, the ability of the wall material (TSM) to retain and protect the core material (SO) was increased, resulting in a higher encapsulation efficiency. Similar trends have been found for other wall material encapsulating seed oils, as cactus mucilage (surface oil 10% and 26% and encapsulation efficiency 90% and 43%, respectively) [26], chia seed mucilage (surface oil 6.1% and 8.4% and encapsulation efficiency 96.7% and 95.1%, respectively) [27], brea gum (surface oil 9.5% and 29.75% and encapsulation efficiency 76.12% and 37.48%, respectively) [33].

3.4.2. Lipid oxidation by peroxide value

The oxidative stability of sesame oil using tamarind seed mucilage as wall material is shown in Fig. 4. All samples were stored six weeks at 25, 35 and 40 °C and water activities of 0.329, 0.318 and 0.313. The results show the formation of peroxide on free sesame seed oil (SO) and sesame seed oil encapsulated employing tamarind seed mucilage (TSM-SO). For all temperatures, the stability of the peroxide value for free oil was considerably lower than for microcapsules M1 and M2, also the stability was increased with encapsulation efficiency (M1 > M2). This effect was reported by Lehn et al. [26]. Also, Yang [34] found that the microcapsules structure was improved by increasing the wall material quantity and the encapsulation efficiency, ending up with an improvement on the oxidative stability of the microcapsules.

The peroxide value of sesame seed oil before microencapsulation was 5.09 ± 0.42 peroxide mEq/oil kg, while for microcapsules after spray drying were 5.13 ± 0.16 peroxide mEq/oil kg for M1 microcapsules, and 5.19 ± 0.24 peroxide mEq/oil kg for M2 microcapsules. The values for free and encapsulated oil were too similar with no significant differences ($P > 0.05$) between different core-to-wall formulations. In this way, the results indicated that the emulsification and encapsulation processes did not exert a negative impact on the oxidative degradation of sesame seed oil (SO).

Independent of temperature, after six weeks of storage, the PV of the free oil rapidly increased and reached to maximum values of 28.83, 29.16 and 29.66 mEq/kg oil at 25, 34 and 40 °C, respectively. On the other hand, the microcapsules M1 and M2 followed a similar oxidation pattern, presenting lower oxidative levels, achieving maximum levels at 40 °C and six weeks of storage for M1 of 14.65 mEq/kg oil and for M2 of 16.51 mEq/kg oil. The variation of oil load in microcapsules having different core-to-wall ratio also affected the oxidative stability of the encapsulated oil. This effect was more visible for M2 with higher PV than in M1. This fact can be attributed to the amount of oil present on the surface of microcapsules since a higher surface oil allows higher peroxide formation. It has been reported that higher oil concentration in microcapsules leads to higher lipid oxidation due to lower encapsulation efficiency and higher surface oil [35].

The thermal influence on PV stability values is observed in Fig. 4. It can be seen that higher temperatures boost the formation of peroxides, either, due to the initiation, propagation step and the decomposition of hydroperoxyl radicals. These oxidative reactions involving PUFAs lead to unacceptable sensory issues for consumers, loss in nutritional value and may sometime cause health disorders [36]. A similar phenomenon was observed for chia seed oil [19]. Regarding the effect of the storage time, the peroxide values of the microcapsules reached the limit set for human consumption according to the CODEX Alimentarius Commission, which is established to be lower than 10 mEq/oil kg [37]. The limit for free SO was achieved at first week of storage, independently of temperature, for M1 microcapsules at fourth week (for 25 and 35 °C) and third week (for 40 °C), whereas that for M2 microcapsules at fourth week (for 25 °C) and third week (for 35 and 40 °C). Hence, the introduction of tamarind seed mucilage as a wall material for encapsulation

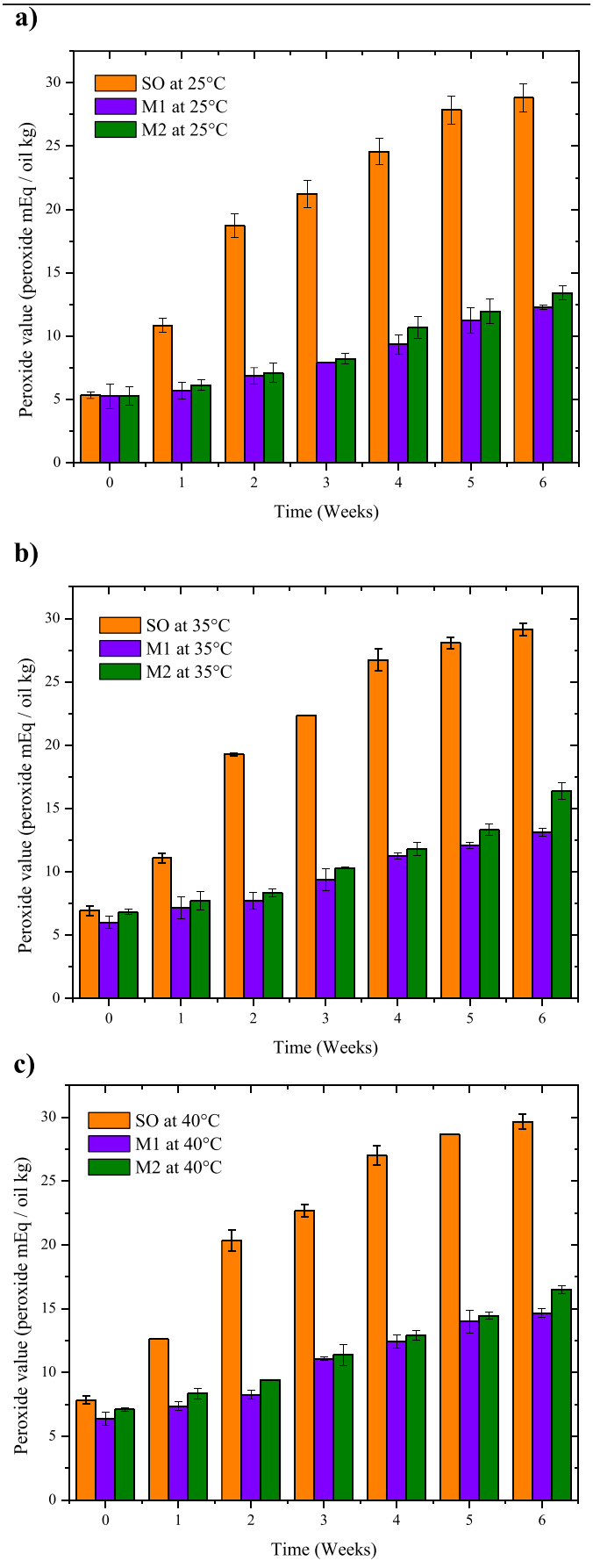

Fig. 4. Oxidation of TSM-SO microcapsules at a) 25, b) 35 and c) 40 °C.

corroborates the viability when protecting oils susceptible to oxidation processes.

The results described above showed that the TSM provided an effective protection against oxidation during the storage of SO. The protection against oil oxidation is a function of the properties of the wall material used. The wall system is designed to provide protection against transport phenomena between the inner part of the microcapsule and the environment [26].

3.5. Morphology and size of microcapsules

3.5.1. Morphology by SEM

Microcapsules were evaluated by SEM to analyze shape and surface features (Fig. 5). The surface analysis of the microcapsules revealed semi-spherical shapes, with continuous walls and no apparent fissures or cracks. Moreover, some of the particles presented concave and shrivelled surfaces, which is typical of microcapsules produced by the spray drying process in the atomizer [8]. The morphology of these microcapsules was found to vary according to the number of wall materials used in their production. However, they all seemed to be almost spherical in shape with a size found to be diversified mostly in the range of 5–12.5 μm for M1 and 5–50 μm for M2 in diameter. It is possible to observe some differences between M1 and M2. Microcapsules M2 containing highest wall material:core ratio appeared to show the formation of some clusters, even agglomerations. This fact is attributed to high amounts of surface oil present on microcapsules. In contrast, microcapsules prepared with less wall material:core ratio (M1) presented discrete particles by both smooth and wrinkled surfaces, with a skin-like structure or polymeric appearance, a phenomenon widely observed on spray-dried microcapsules employing low ratios on wall material: core conformation.

3.5.2. Particle size distribution

The particle size distribution (Fig. 6) of M1 exhibited a unimodal character, with sizes ranged from ~1 to 50 μm. Meanwhile, the distribution of M2 microcapsules showed a bimodal character, which might be associated with the higher oil content on the surface of microcapsules allowing the conformation of agglomerates between powder particles of microcapsules [38]. Mean particle diameter $D_{[4,3]}$, indicates substantial increments on values for microcapsules with less sesame oil content (M1) from 11.40 to 48.1 μm for higher amounts of sesame oil (M2). These differences might be attributed to the predominance of oil molecules all over the system, and a subsequent lack of TSM molecules able to cover up the oil droplets, thus allowing the formation of bigger microcapsule particles [36]. Similar behavior on mean particle size distribution studies was observed with microcapsules formulated employing chia mucilage [39] and nopal mucilage [40].

4. Conclusions

The present study revealed the possibility of encapsulating sesame seed oil by spray drying using tamarind seed mucilage as a wall material achieving high-efficiency values and delaying oxidation mechanisms of oil. A characteristic feature is the use of higher relations Wm:Co than commonly used on microencapsulation of 1:1 and 1:2, for M1 and M2, respectively. Encapsulation efficiency presented greater values for M1 microcapsules (91.05%) than to M2 (81.22%) microcapsules. Hence, the most ideal system among this study was M1, leading to the optimal encapsulation efficiency for the microencapsulation of SO with the lowest proportion of surface oil. For all temperatures, the stability of the peroxide value was increased with encapsulation efficiency (M1 > M2). The variation of oil load in microcapsules having different core-to-wall ratio also affected the oxidative stability of the

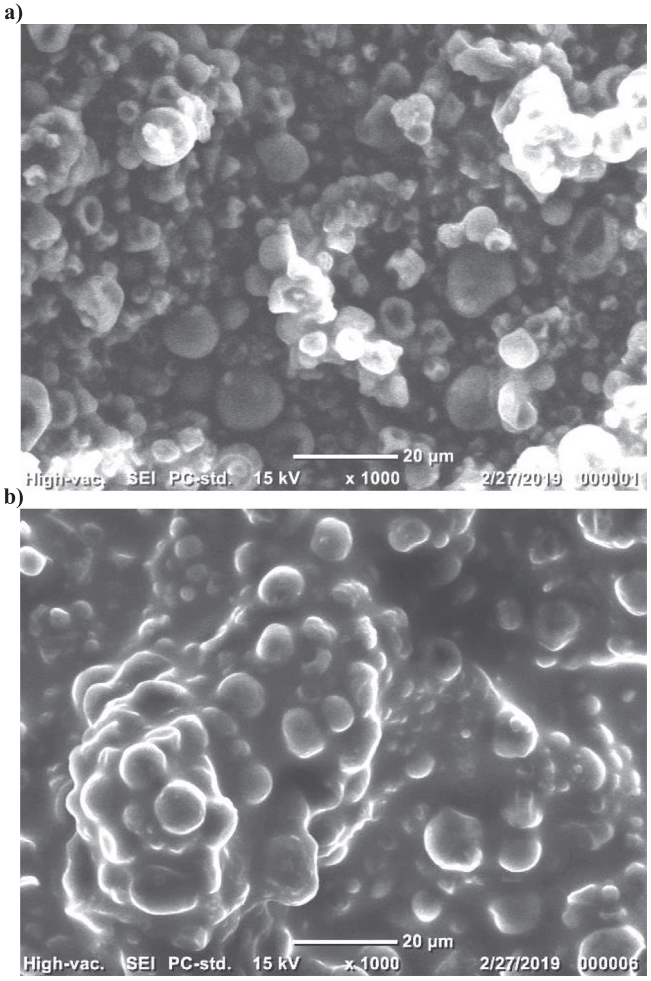

Fig. 5. Morphology by SEM of a) M1 and b) M2 microcapsules at 1000×.

encapsulated oil, this effect was greater in M2 with higher PV than in M1, because, a higher surface oil allows peroxides formation. The limit of peroxides set for human consumption free SO was achieved at the first week of storage and M1 and M2 microcapsules was reached at the fourth week. These results clearly showed that the TSM used on the microencapsulation process as a new wall material provided an effective protection against oxidation during the storage of SO. The introduction of tamarind seed mucilage (TSM) as a wall material for encapsulation, corroborates the manageability, thermal stability, efficiency, and viability when protecting oils susceptible to oxidation processes, even though, when encapsulating high amounts of oil.

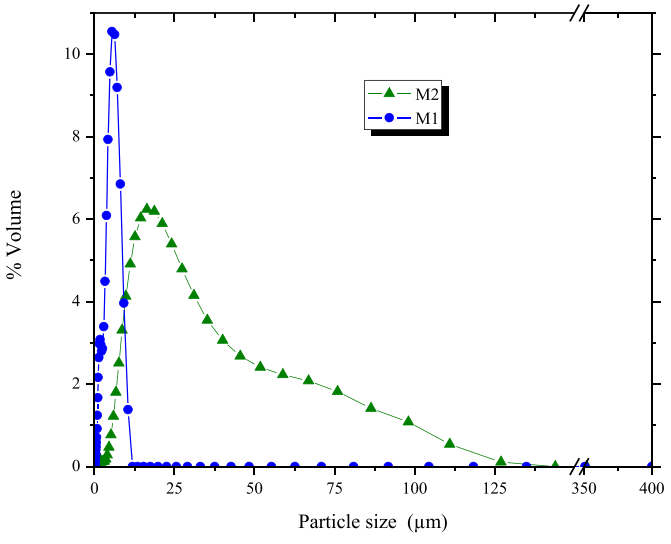

Fig. 6. Mean size distributions for TSM-SO microcapsules.

CRediT authorship contribution statement

Erik Alpizar-Reyes: Conceptualization, Methodology, Software, Validation, Formal analysis, Investigation, Data curation, Writing - original draft, Writing - review & editing, Visualization, Supervision, Project administration. **Victor Varela-Guerrero:** Conceptualization, Investigation, Resources, Visualization, Supervision, Project administration. **Julian Cruz-Olivares:** Conceptualization, Resources, Writing - original draft, Project administration, Funding acquisition. **Héctor Carrillo-Navas:** Validation, Formal analysis, Writing - original draft, Writing - review & editing, Resources. **Jose Alvarez-Ramirez:** Conceptualization, Writing - original draft, Writing - review & editing, Visualization, Supervision. **César Pérez-Alonso:** Conceptualization, Resources, Data curation, Writing - original draft, Writing - review & editing, Visualization, Supervision, Project administration, Funding acquisition.

Acknowledgements

The authors wish to acknowledge the partial financial support of this research to the Universidad Autónoma del Estado de México through project 4371/2017/CI.

Declaration of competing interest

The authors declare that there is no conflict of interest relating to the publication of this article.

References

[1] E. Burnside, Hydrocolloids and gums as encapsulating agents, Microencapsul. Food Ind. Elsevier 2014, pp. 241–252, https://doi.org/10.1016/B978-0-12-404568-2.00021-2.
[2] B.N. Estevinho, F. Rocha, Microencapsulation Processes - YouTube, Elsevier Inc, 2018https://doi.org/10.1016/B978-0-12-811449-0/00007-4.
[3] D. Saha, S. Bhattacharya, Hydrocolloids as thickening and gelling agents in food: a critical review, J. Food Sci. Technol. 47 (2010) 587–597, https://doi.org/10.1007/s13197-010-0162-6.
[4] P. Varela, S.M. Fiszman, Hydrocolloids in fried foods. A review, Food Hydrocoll. 25 (2011) 1801–1812, https://doi.org/10.1016/j.foodhyd.2011.01.016.
[5] C. Soukoulis, C. Gaiani, L. Hoffmann, Plant seed mucilage as emerging biopolymer in food industry applications, Curr. Opin. Food Sci. 22 (2018) 28–42, https://doi.org/10.1016/j.cofs.2018.01.004.
[6] E. Alpizar-Reyes, H. Carrillo-Navas, R. Gallardo-Rivera, V. Varela-Guerrero, J. Alvarez-Ramirez, C. Pérez-Alonso, Functional properties and physicochemical characteristics of tamarind (Tamarindus indica L.) seed mucilage powder as a novel hydrocolloid, J. Food Eng. 209 (2017) 68–75, https://doi.org/10.1016/j.jfoodeng.2017.04.021.
[7] E. Alpizar-Reyes, A. Román-Guerrero, R. Gallardo-Rivera, V. Varela-Guerrero, J. Cruz-Olivares, C. Pérez-Alonso, Rheological properties of tamarind (Tamarindus indica L.) seed mucilage obtained by spray-drying as a novel source of hydrocolloid, Int. J. Biol. Macromol. 107 (2018) 817–824, https://doi.org/10.1016/j.ijbiomac.2017.09.048.
[8] E. Alpizar-Reyes, H. Carrillo-Navas, R. Romero-Romero, V. Varela-Guerrero, J. Alvarez-Ramírez, C. Pérez-Alonso, Thermodynamic sorption properties and glass transition temperature of tamarind seed mucilage (Tamarindus indica L.), Food Bioprod. Process. 101 (2017) 166–176, https://doi.org/10.1016/j.fbp.2016.11.006.
[9] E. Lee, E. Choe, Changes in oxidation-derived off-flavor compounds of roasted sesame oil during accelerated storage in the dark, Biocatal. Agric. Biotechnol. 1 (2012) 89–93, https://doi.org/10.1016/j.bcab.2011.08.003.
[10] D. Xu-Yan, L. Ping-Ping, W. Fang, J. Mu-Lan, Z. Ying-Zhong, L. Guang-Ming, C. Hong, Z. Yuan-Di, The impact of processing on the profile of volatile compounds in sesame oil, Eur. J. Lipid Sci. Technol. 114 (2012) 277–286, https://doi.org/10.1002/ejlt.201100059.
[11] F. Mohseni, S.A.H. Goli, Encapsulation of flaxseed oil in the tertiary conjugate of oxidized tannic acid-gelatin and flaxseed (Linum usitatissimum) mucilage, Int. J. Biol. Macromol. 140 (2019) 959–964, https://doi.org/10.1016/j.ijbiomac.2019.08.197.
[12] Y.P. Timilsena, R. Adhikari, C.J. Barrow, B. Adhikari, Microencapsulation of chia seed oil using chia seed protein isolate-chia seed gum complex coacervates, Int. J. Biol. Macromol. 91 (2016) 347–357, https://doi.org/10.1016/j.ijbiomac.2016.05.058.
[13] N. Jannasari, M. Fathi, S.J. Moshtaghian, A. Abbaspourrad, Microencapsulation of vitamin D using gelatin and cress seed mucilage: production, characterization and

in vivo study, Int. J. Biol. Macromol. 129 (2019) 972–979, https://doi.org/10.1016/j.ijbiomac.2019.02.096.
[14] M.D.P. Farias, P.B.S. Albuquerque, P.A.G. Soares, D.M.A.T. de Sá, A.A. Vicente, M.G. Carneiro-da-Cunha, Xyloglucan from Hymenaea courbaril var. courbaril seeds as encapsulating agent of L-ascorbic acid, Int. J. Biol. Macromol. 107 ((2018) 1559–1566, https://doi.org/10.1016/j.ijbiomac.2017.10.016.
[15] K. Manoi, S.S.H. Rizvi, Emulsification mechanisms and characterizations of cold, gel-like emulsions produced from texturized whey protein concentrate, Food Hydrocoll. 23 (2009) 1837–1847, https://doi.org/10.1016/j.foodhyd.2009.02.011.
[16] P. Kalegowda, A.S. Chauhan, S. Mysore, N. Urs, Opuntia dillenii (Ker-Gawl) Haw cladode mucilage: physico-chemical, rheological and functional behavior, Carbohydr. Polym. 157 (2017) 1057–1064, https://doi.org/10.1016/j.carbpol.2016.10.070.
[17] AOAC, Official Methods of Analysis of AOAC International, 2006 534.
[18] D.A. Rodea-González, J. Cruz-Olivares, A. Román-Guerrero, M.E. Rodríguez-Huezo, E.J. Vernon-Carter, C. Pérez-Alonso, Spray-dried encapsulation of chia essential oil (Salvia hispanica L.) in whey protein concentrate-polysaccharide matrices, J. Food Eng. 111 (2012) 102–109, https://doi.org/10.1016/j.jfoodeng.2012.01.020.
[19] L.A. Escalona-García, R. Pedroza-Islas, R. Natividad, M.E. Rodríguez-Huezo, H. Carrillo-Navas, C. Pérez-Alonso, Oxidation kinetics and thermodynamic analysis of chia oil microencapsulated in a whey protein concentrate-polysaccharide matrix, J. Food Eng. 175 (2016) 93–103, https://doi.org/10.1016/j.jfoodeng.2015.12.009.
[20] F. Niu, D. Niu, H. Zhang, C. Chang, L. Gu, Y. Su, Y. Yang, Ovalbumin/gum arabic-stabilized emulsion: rheology, emulsion characteristics, and Raman spectroscopic study, Food Hydrocoll. 52 (2016) 607–614, https://doi.org/10.1016/j.foodhyd.2015.08.010.
[21] D.J. Mcclements, Food Emulsions: 2. Molecular Interactions, Interactions, 1999.
[22] S.C. Chew, C.P. Tan, K.L. Nyam, Microencapsulation of refined kenaf (Hibiscus cannabinus L.) seed oil by spray drying using β-cyclodextrin/gum arabic/sodium caseinate, J. Food Eng. 237 (2018) 78–85, https://doi.org/10.1016/j.jfoodeng.2018.05.016.
[23] A. Goyal, V. Sharma, M.K. Sihag, S.K. Tomar, S. Arora, L. Sabikhi, A.K. Singh, Development and physico-chemical characterization of microencapsulated flaxseed oil powder: a functional ingredient for omega-3 fortification, Powder Technol. 286 (2015) 527–537, https://doi.org/10.1016/j.powtec.2015.08.050.
[24] C. Turchiuli, M. Fuchs, M. Bohin, M.E. Cuvelier, C. Ordonnaud, M.N. Peyrat-Maillard, E. Dumoulin, Oil encapsulation by spray drying and fluidised bed agglomeration, Innov. Food Sci. Emerg. Technol. 6 (2005) 29–35, https://doi.org/10.1016/j.ifset.2004.11.005.
[25] J. Vongsvivut, P. Heraud, W. Zhang, J.A. Kralovec, D. McNaughton, C.J. Barrow, Quantitative determination of fatty acid compositions in micro-encapsulated fish-oil supplements using Fourier transform infrared (FTIR) spectroscopy, Food Chem. 135 (2012) 603–609, https://doi.org/10.1016/j.foodchem.2012.05.012.
[26] D.N. Lehn, V.M. Esquerdo, M.A. Dahlem Júnior, W. Dall'Agnol, A.C.F. dos Santos, C.F.V. de Souza, L.A. de Almeida Pinto, Microencapsulation of different oils rich in unsaturated fatty acids using dairy industry waste, J. Clean. Prod. 196 (2018) 665–673, https://doi.org/10.1016/j.jclepro.2018.06.127.
[27] Y.P. Timilsena, J. Vongsvivut, M.J. Tobin, R. Adhikari, C. Barrow, B. Adhikari, Investigation of oil distribution in spray-dried chia seed oil microcapsules using synchrotron-FTIR microspectroscopy, Food Chem. 275 (2019) 457–466, https://doi.org/10.1016/j.foodchem.2018.09.043.
[28] K. Sudarshan, S. Karthikeyan, P. Maria jenita, U. Lalitha priya, V. Renuka, K. Harini, S. Babuskin, M. Sukumar, B. Vajiha Aafrin, C. Chandra Mohan, Extraction and characterization of polysaccharides from tamarind seeds, rice mill residue, okra waste and sugarcane bagasse for its bio-thermoplastic properties, Carbohydr. Polym. 186 (2018) 394–401, https://doi.org/10.1016/j.carbpol.2018.01.057.
[29] A. Kozioł, J. Cybulska, P.M. Pieczywek, A. Zdunek, Evaluation of structure and assembly of xyloglucan from tamarind seed (Tamarindus indica L.) with atomic force microscopy, Food Biophys. 10 (2015) 396–402, https://doi.org/10.1007/s11483-015-9395-2.
[30] L. Hu, J. Zhang, Q. Hu, N. Gao, S. Wang, Y. Sun, X. Yang, Microencapsulation of brucea javanica oil: characterization, stability and optimization of spray drying conditions, J. Drug Deliv. Sci. Technol. 36 (2016) 46–54, https://doi.org/10.1016/j.jddst.2016.09.008.
[31] M.T.H. Swe, P. Asavapichayont, Effect of silicone oil on the microstructure, gelation and rheological properties of sorbitan monostearate–sesame oil oleogels, Asian J. Pharm. Sci. 13 (2018) 485–497, https://doi.org/10.1016/j.ajps.2018.04.006.
[32] A. Gharsallaoui, G. Roudaut, O. Chambin, A. Voilley, R. Saurel, Applications of spray-drying in microencapsulation of food ingredients: an overview, Food Res. Int. 40 (2007) 1107–1121, https://doi.org/10.1016/J.FOODRES.2007.07.004.
[33] V. Castel, A.C. Rubiolo, C.R. Carrara, Brea gum as wall material in the microencapsulation of corn oil by spray drying: effect of inulin addition, Food Res. Int. 103 (2018) 76–83, https://doi.org/10.1016/j.foodres.2017.10.036.
[34] X. Yang, Influences of preparation conditions on the formation and depth dispersion of Ag nanoparticles in soda-lime silicate glass, J. Non-Cryst. Solids 430 (2015) 87–93, https://doi.org/10.1016/j.jnoncrysol.2015.09.028.
[35] R.V. Tonon, C.R.F. Grosso, M.D. Hubinger, Influence of emulsion composition and inlet air temperature on the microencapsulation of flaxseed oil by spray drying, Food Res. Int. 44 (2011) 282–289, https://doi.org/10.1016/j.foodres.2010.10.018.
[36] N.A. Avramenko, C. Chang, N.H. Low, M.T. Nickerson, Encapsulation of flaxseed oil within native and modified lentil protein-based microcapsules, Food Res. Int. 81 (2016) 17–24, https://doi.org/10.1016/j.foodres.2015.12.028.
[37] C. Stan, Codex Almentarius Standart for Edible Fats and Oils, 1999 2–7.
[38] S. Shamaei, S.S. Seiiedlou, M. Aghbashlo, E. Tsotsas, A. Kharaghani, Microencapsulation of walnut oil by spray drying: effects of wall material and drying conditions on physicochemical properties of microcapsules, Innov. Food Sci. Emerg. Technol. 39 (2017) 101–112, https://doi.org/10.1016/j.ifset.2016.11.011.
[39] M.I. Capitani, S.M. Nolasco, M.C. Tomás, Stability of oil-in-water (O/W) emulsions with chia (Salvia hispanica L.) mucilage, Food Hydrocoll. 61 (2016) 537–546, https://doi.org/10.1016/j.foodhyd.2016.06.008.
[40] C. Quinzio, C. Ayunta, B. López de Mishima, L. Iturriaga, Stability and rheology properties of oil-in-water emulsions prepared with mucilage extracted from Opuntia ficus-indica (L). Miller, Food Hydrocoll. 84 (2018) 154–165, https://doi.org/10.1016/j.foodhyd.2018.06.002.